Adv. Space Res. Vol. 13, No. 5, pp. (5)167–(5)176, 1993
Printed in Great Britain.

0273–1177/93 $24.00
1993 COSPAR

INTERCOMPARISONS BETWEEN PASSIVE AND ACTIVE MICROWAVE REMOTE SENSING, AND HYDROLOGICAL MODELING FOR SOIL MOISTURE

E. F. Wood,* D. -S. Lin,* M. Mancini,* D. Thongs,*
P. A. Troch,* T. J. Jackson,** J. S. Famiglietti*
and E. T. Engman***

** Department of Civil Engineering and Operations Research, Princeton University, Princeton, NJ 08544, U.S.A.*
*** USDA-ARS Hydrology Laboratory, Beltsville, MD 20705, U.S.A.*
**** NASA, Goddard Space Flight Center, Greenbelt, MD 20771, U.S.A.*

ABSTRACT

Soil moisture estimates from a distributed hydrological model and two microwave remote sensors (Push Broom Microwave Radiometer and Synthetic Aperture Radar) were compared with the ground measurements collected during the MAC-HYDRO'90 experiment over a 7.4-km^2 watershed in central Pennsylvania. Various information, including rainfall, soil properties, land cover, topography and remote sensing imagery, were integrated and analyzed using an image integration technique. It is found that the hydrological model and both microwave sensors successfully pick up the temporal variation of soil moisture. Results also indicate the spatial soil moisture pattern can be remotely sensed within reasonable accuracy using existing algorithms. Watershed averaged soil moisture estimates from the hydrological model are wetter than remotely sensed data. It is difficult to conclude which instrument yield better performance for the studied case. The choice will be based on the intended applications and information that is available.

INTRODUCTION

Knowledge of soil moisture distribution in space and time is of considerable importance for many hydrological and agricultural applications. As a result of the inhomogeneity of soil properties, topography, land cover, and precipitation, soil moisture is highly variable both spatially and temporally. Soil moisture estimation has been based on extrapolation of point measurements. Recent advances in microwave remote sensing have demonstrated the ability to measure surface soil moisture, in the order of 5 cm, under a variety of topographic and land cover conditions (Engman, 1990).

Despite the promising perspective of this new technique, its application to agricultural and hydrological sciences has been slow. This is because most existing hydrological models are formulated on point processes. These models are not capable of using the remotely sensed data as direct input or to verify output.

This paper compares remotely sensed and model simulated soil moisture with ground observations using the data collected in an experiment conducted in the summer of 1990 (MAC-HYDRO'90). The spatially-distributed hydrological model proposed by Paniconi and Wood (1992) is used for simulations. The purpose of this study is to evaluate the performance of the hydrological model and to examine the limitations of various remote sensing techniques used in soil moisture estimation. Results will be used to investigate future directions for incorporation of the remotely sensed data into hydrological models.

Site Description

MAC-HYDRO'90 was conducted over a portion of the Mahantango Creek which is a 7.4-km^2 research watershed operated by the Northeast Watershed Research Center of the USDA, ARS in Pennsylvania. The climate of this area is considered as temperate and humid. The average annual precipitation and evapotranspiration for the watershed are 1128 mm and 479 mm per year, respectively. The intensive study area includes a subwatershed (WD38) of about 50 ha on the eastern portion of the larger area (see Figure 1). The 50-ha subwatershed is nearly all cropped (corn, wheat, oats, and hay) and is bounded on the south by forest. The soils within this region are primarily silt loams and loams, and contain 0.5 $\sim$ 2.0 % organic carbon. Within the studied watershed, 15 different soil types can be identified. These soils have similar hydraulic properties (Troch et al., 1992).

Weather Conditions

The weather conditions for the experiment were dry initially. No rain was recorded during the preceding 5 days, resulting in uniformly dry soil conditions. After the first flight (July 10, 1990), there was an approximately 52 mm of rainfall over a four-day period, followed by a strong dry down. These conditions generated a wide range of soil moisture conditions which provide an excellent test ground for remote sensors and allow for intercomparisons among various data. The rainfall record and the dates of data collections are tabulated in Table 1.

Ground Data

Two kinds of soil sampling strategies were used. For large homogeneous agricultural fields, samples were taken from a grid to provide a field averaged soil moisture value. In addition, samples were collected along transects which were aligned at right angles to the streams. Samples were taken at two depths, 0 $\sim$ 5 cm and 5 $\sim$ 10 cm and consisted of 5 cm^3 in volume. The location of some sampling sites and raingage network is shown in Figure 1.

Land cover information was compiled for a large area and was classified into 9 categories (see Figure 2). Rainfall records were collected from a network of 15 tipping-bucket raingages deployed over the watershed. A micrometeorological station located near the center of the catchment provide the time series of meteorological variables.

Passive Microwave Radiometer

The passive microwave instrument used in this campaign was the push broom microwave radiometer (PBMR). The PBMR operates at L-band (f = 1.42 GHz). It has four horizontally polarized beams pointing at $\pm 8°$ and $\pm 24°$ from nadir. The field of view is 1.2 times the altitude which was 300 m in MACHYDRO'90. For a detailed description of the PBMR, see Schmugge et al. (1988).

Data collected from the PBMR were processed following procedures that have been successfully employed in previous experiments (Schmugge et al., 1992). Vegetation corrections are applied to the average brightness temperature maps to estimate soil emissivity (Jackson and Schmugge, 1991). Dielectric constants of soils are calculated from soil emissivity using Fresnel's formulae. Knowing the soil dielectric constants, a semi-empirical dielectric mixing model (Dobson et al., 1985) is used to estimate the volumetric soil moisture.

Synthetic Aperture Radar

Aircraft radar data were acquired at multiple angles over the Mahantango Creek using the Jet Propulsion Laboratory multipolarization imaging radar (AIRSAR) in three frequencies (f = 0.44, 1.25 and 5.33 GHz).

TABLE 1. MAC-HYDRO'90 Data Collection.

Date	Rainfall Accumulation (mm)	PBMR	SAR	Ground Data
July 10	0	Yes	Yes	Yes
July 13	39	No	Yes	Yes
July 15	52	Yes	Yes	Yes
July 17	52	Yes	Yes	Yes
July 18	52	Yes	No	Yes
July 19	52	Yes	No	Yes
July 20	52	No	No	Yes

For a detailed description of the instrument, see Held et al. (1988). Three flight lines were flown each day with the objective of obtaining various incidence angles (20°, 30° and 45°) of the target area (76°35′ W, 40°43′ N). On July 15 and 17, high resolution data with a 3.331 m slant range pixel size were also taken.

The AIRSAR imagery were calibrated for phase, cross-talk, channel imbalance and absolute power using trihedral corner reflectors. The underlying theories and algorithms for signal calibrations are presented in van Zyl et al. (1990). The calibrated SAR imagery are then registered with the USGS 7.5-min digital elevation model (DEM), giving the local incidence angle of each pixel.

Hydrological Model

The hydrological model predicts patterns of soil saturation and their relationship to both saturation excess and infiltration excess surface runoff generation by solving the three-dimensional Richards equation numerically (Paniconi and Wood, 1992). Richards equation with pressure head ψ as the dependent variable can be written as

$$S(\psi)\frac{\partial \psi}{\partial t} = \nabla \cdot [K_s K_r(\psi)\nabla(\psi + z)] \tag{1}$$

where t is time, z is the vertical coordinate, positive upward, and the hydraulic conductivity is expressed as a product of the conductivity at saturation, K_s, and the relative conductivity, K_r. An extension of the van Genuchten characteristic equations (van Genuchten and Nielsen, 1985) is used to describe the nonlinear relationships of volumetric moisture content θ, specific moisture capacity S, relative hydraulic conductivity K_r and the pressure head. Notice that hysteresis effects on moisture redistribution are not taken into account.

The initial water table depth for each pixel is computed using the procedure developed by Troch et al. (1992). The lower and lateral boundaries are assumed impervious. According to the geological records, the location of lower boundary is held fixed at 5 m below surface.

RESULTS AND DISCUSSION

Some large agricultural fields were used as verification sites to test the performance of instruments before the comparisons are performed.

Verification Sites

Four corn fields located east of the main watershed are chosen for verification purposes (see Figure 2). Data collected over these fields are also used to develop inversion algorithm for SAR. These corn fields are the largest accessible agricultural fields in the area. During the experiment, corn stood approximately 90 cm in height and contained 2 kg/m^2 of water.

TABLE 2. Results of Linear Regression Analysis.

Canopy	Band	Polarization	Slope	Intercept	r
Corn	L	HH	2.625	50.986	0.783
Corn	L	VV	0.979	32.666	0.525
Corn	L	HV	3.329	95.786	0.827
Corn	C	HH	4.374	55.670	0.730
Corn	C	VV	4.915	64.454	0.837
Corn	C	HV	7.097	131.298	0.863
Oat	L	HH	3.672	89.835	0.805
Oat	L	VV	3.481	87.214	0.908
Oat	L	HV	1.800	74.185	0.590
Oat	C	HH	3.403	48.377	0.831
Oat	C	VV	3.298	61.623	0.894
Oat	C	HV	3.411	82.146	0.657
Pasture	L	HH	4.792	92.029	0.642
Pasture	L	VV	5.161	95.083	0.909
Pasture	L	HV	3.894	130.767	0.471
Pasture	C	HH	0.552	39.933	0.821
Pasture	C	VV	1.002	48.379	0.633
Pasture	C	HV	9.559	199.410	0.884

Figure 3 displays the temporal variation of the PBMR brightness temperature and the L-band HH-polarization SAR signal averaged over the corn fields 1 and 2 during the course of the experiment. Volumetric soil moisture contents from ground measurements are also plotted in the figure for references. It can be seen from the figure that the brightness temperatures measured by the PBMR decrease with increasing soil wetness. Meanwhile, stronger SAR backscattering signal was observed on wet days. In general, both sensors have reflected the temporal variation of soil moisture on these large corn fields pretty well.

Most existing SAR inversion algorithms are designed for bare soil surfaces (Soares et al., 1991; Oh et al., 1992). Pultz et al. (1990) have presented an estimation scheme for wheat and canola using field data collected in Canada. However, as pointed out by the authors, those relationships are site specific. It is, therefore, decided to develop empirical relationships for the MAC-HYDRO'90 site. Signals from four corn fields, two oat field and three pasture areas were extracted and linearly regressed with corresponding 0~5 cm ground soil moisture measurements. Results of the regression analysis are summarized in Table 2.

It appears that no particular combination of wavelength and polarization yield decisive edge. Considering the fact that it is more difficult to calibrate cross-polarization signal than like-polarization signal, we have decided to use the C-band VV-polarization signal to estimate soil moisture for all corn fields in watershed. For pasture and oat fields, the L-band VV-polarization signal will be used. These estimated regression relationships are shown in Figure 4. It is noted that the ranges of validity of these empirical relationships are limited. Extrapolation of the regression equations could lead to significant errors.

Subwatershed

To estimate watershed soil moisture from the PBMR brightness temperature, we apply the vegetation correction over the area in four categories: corn (38%), small grains (28%), pasture (14%) and hay (13%). Forest (6%) and residential area (1%) are excluded from the computation because the microwave signals are not related to soil moisture under these situations. The vegetation biomass for each category has been estimated from field samples or from previous data.

TABLE 3. Regional Volumetric Soil Moisture Estimates for the WD38 Subwatershed.

Date	PBMR (%)	SAR (%)	Model (%)	Ground (%)
July 10	13	14.5	28	12.0
July 13	-	22.9	38	25.1
July 15	23	24.0	36	25.0
July 17	26	25.1	33	22.8
July 18	19	-	32	20.8
July 19	19	-	30	19.7
July 20	-	-	26	17.5

For the case of the SAR, pasture and hay are treated as the same. Forest and residential area are excluded from the computation for the same reason described above. The following regression equations are used for soil moisture estimation,

$$M_v = \begin{cases} 64.454 + 4.915\ \sigma^0_{CVV}, & for\ Corn \\ 87.214 + 3.481\ \sigma^0_{LVV}, & for\ Small\ grains \\ 95.083 + 5.161\ \sigma^0_{LVV}, & for\ Pasture\ and\ hay \end{cases} \quad (2)$$

where M_v is volumetric soil moisture content in %, σ^0_{CVV} and σ^0_{LVV} are the VV-polarization backscattering coefficients in dB for C-band and L-band, respectively. It should be noted that, in order to reduce signal noises, field averaged signals are used in the above relationships.

The average soil moisture values over the WD38 subwatershed derived from the PBMR, the SAR and the hydrological model are listed in Table 3. The ground observations were averages of approximately 60 ground samples except on July 15 when only 33 were taken. The estimates between the PBMR and the ground measurements are in good agreement. This implies that the PBMR average procedure is quite successful in this case. Estimates from the hydrological model are wetter than other observations. The temporal variation, however, is correct. The cause for this bias is currently under study. Despite using the rather crude empirical relationships, the SAR is able to predict watershed averaged soil moisture values within 20 % of the ground measurements.

Finally, it is difficult to compare the performances of passive and active microwave instruments under the current circumstance. The fine resolution of the SAR was partly diminished when field averaged soil moisture. In addition, The SAR requires additional topographic information than the PBMR. On the other hand, geo- referencing of the PBMR measurements is an involved work and is subject to large uncertainties for a small agricultural watershed, especially for a small watershed such as Mahantango Creek. The decision of which instrument should be used should depend on available information, as well as the data resolution required for the intended applications.

SUMMARY

The intercomparisons between hydrological model and microwave sensors were conducted over a small watershed in central Pennsylvania. Results can be summarized as follow,

(1) The temporal variation of soil moisture patterns over the verification sites was successfully picked up by both passive and active microwave sensors.

(2) Both microwave instruments yield soil moisture estimates within 20 % of the ground measurements. Soil moisture estimates from the hydrological model are wetter than observations during the MAC- HYDRO'90 period. The choice of an appropriate instrument will depend on the intended applications and available information.

ACKNOWLEDGEMENTS

The authors thank Dr. Bill Teng for supplying the land cover information. The study was partly supported by NASA Global Change Graduate Fellowship (NGT-30049), NASA Grant NAG5-1628 and USDA Cooperative Agreement 58-3K47-0-039 for application of SIR-C Synthetic Aperture Radar to Hydrology. Supports from NASA and USDA are highly appreciated.

REFERENCES

/1/ M.C. Dobson,F.T. Ulaby, M. Hallikasnen and M. El-rayes, *Microwave Dielectric Behavior of Wet Soil-Part II: Dielectric Mixing Models*, IEEE Trans. Geosci. Remote Sen., GE-23, 35-46 (1985).

/2/ E.T. Engman, *Progress in Microwave Remote Sensing of Soil Moisture*, Cana. J. Remote Sensing, vol.16, 6-14 (1990).

/3/ D.N. Held, *The NASA/JPL Multifrequency, Multipolarization Airborne SAR System*, in: Proc. IGARSS'88, Edinburgh, 317-322 (1988).

/4/ T.J. Jackson and T.J. Schmugge, *Vegetation Effects on the Microwave Emission of Soils*, Remote Sensing Env., vol.36, 203-212 (1991).

/5/ Y. Oh, K. Sarabandi and F.T. Ulaby, *An Empirical Model and an Inversion Techniques for Radar Scattering for Bare Soil Surfaces*, IEEE Trans. Geosci. Remote Sens., vol.30, 370-381 (1992).

/6/ C. Paniconi and E.F. Wood, *A Detailed Model for Simulation of Catchment Scale Subsurface Hydrologic Processes*, submitted to Water Resours. Res. (1992).

/7/ T.J. Pultz, R. Leconte, R.J. Brown and B. Brisco, *Quantitative Soil Moisture Extraction from Airborne SAR Data*, Cana. J. Remote Sensing, vol.16, 56-62 (1990).

/8/ J.V. Soares, J.C. Shi, L. Hess, E.T. Engman and J.J. van Zyl, *Estimation of Bare Soil Evaporation From a Multi-Frequency Airborne SAR*, in: 24th Int. Symp. Remote Sens. Env., Rio de Janeiro, Brazil 1991.

/9/ T.J. Schmugge, T.J. Jackson, W.P. Kustas and J.R. Wang, *Passive Microwave Remote Sensing of Soil Moisture: Results from HAPEX, FIFE and MONSOON'90*, J. Photogrammetry Remote Sensing, in press (1992).

/10/ T.J. Schmugge, J.R. Wang and G. Asrar, *Results from the Push Broom Microwave Radiometer Flights over the Konza Prairie in 1985*, IEEE Trans. Geosci. Remote Sens., vol.26, 590-596 (1988).

/11/ P. A. Troch, M. Mancini, C. Paniconi and E.F. Wood, *Evaluation of a Distributed Catchment Scale Water Balance Model*, submitted to Water Resours. Res. (1992).

/12/ M.T. van Genuchten and D.R. Nielsen, *On Describing and Predicting the Hydraulic Properties of Unsaturated Soils*, Ann. Geophys., vol.3, 615-628 (1985).

/13/ J.J. van Zyl, C.F. Burnette, H.A. Zebker, A. Freeman and J. Holt, *POLCAL User's Manual*, JPL, Cal. Tech., Pasadena, CA (1990).

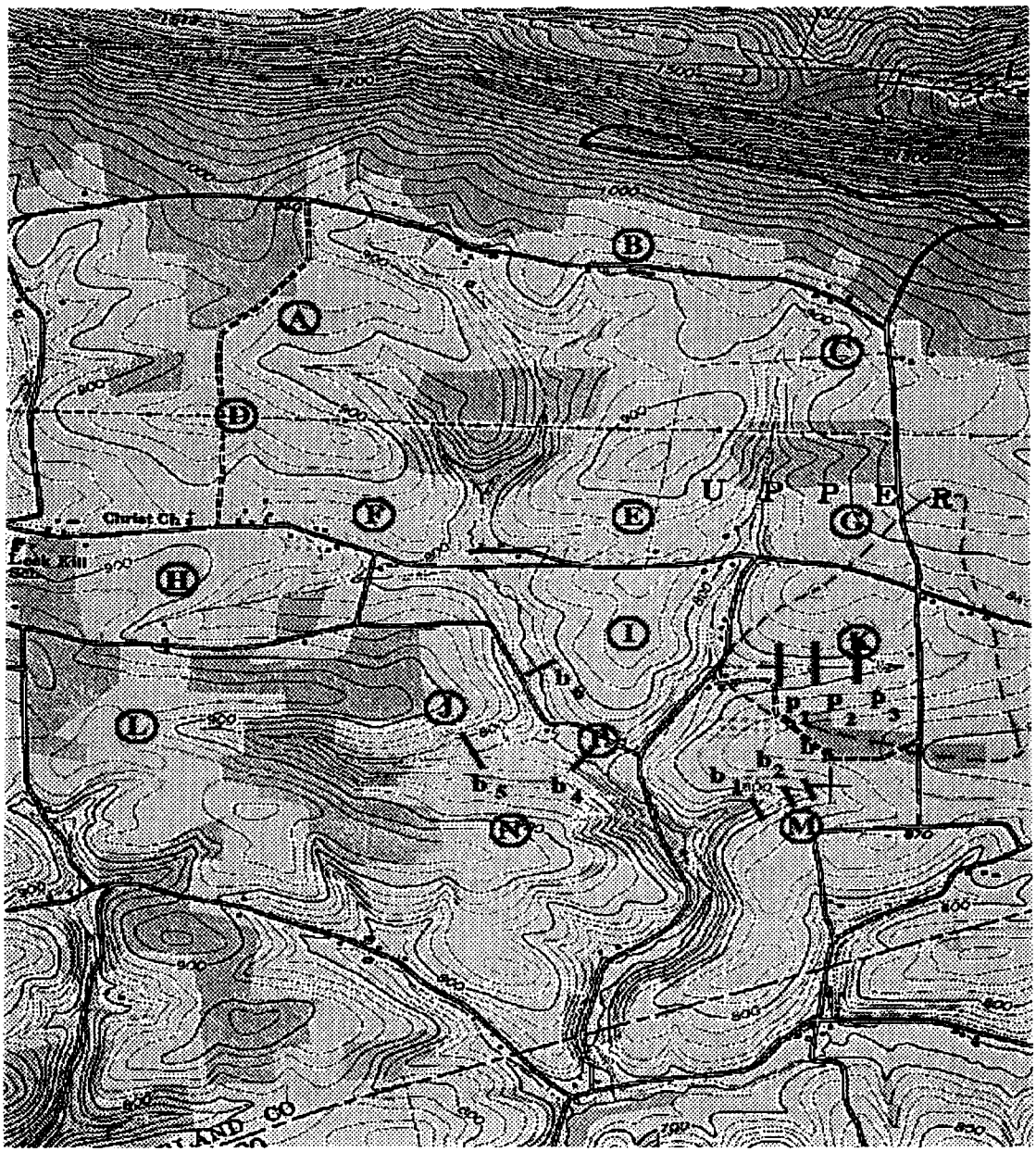

Figure 1: Topography map for MACHYDRO'90 showing some sampling sites and WD38 sub-catchment. P_1 to P_3, B_1 to B_6 are transects along which soil samples are taken.

Figure 2: Land cover map for the studied area derived from aerial photos and field observations.

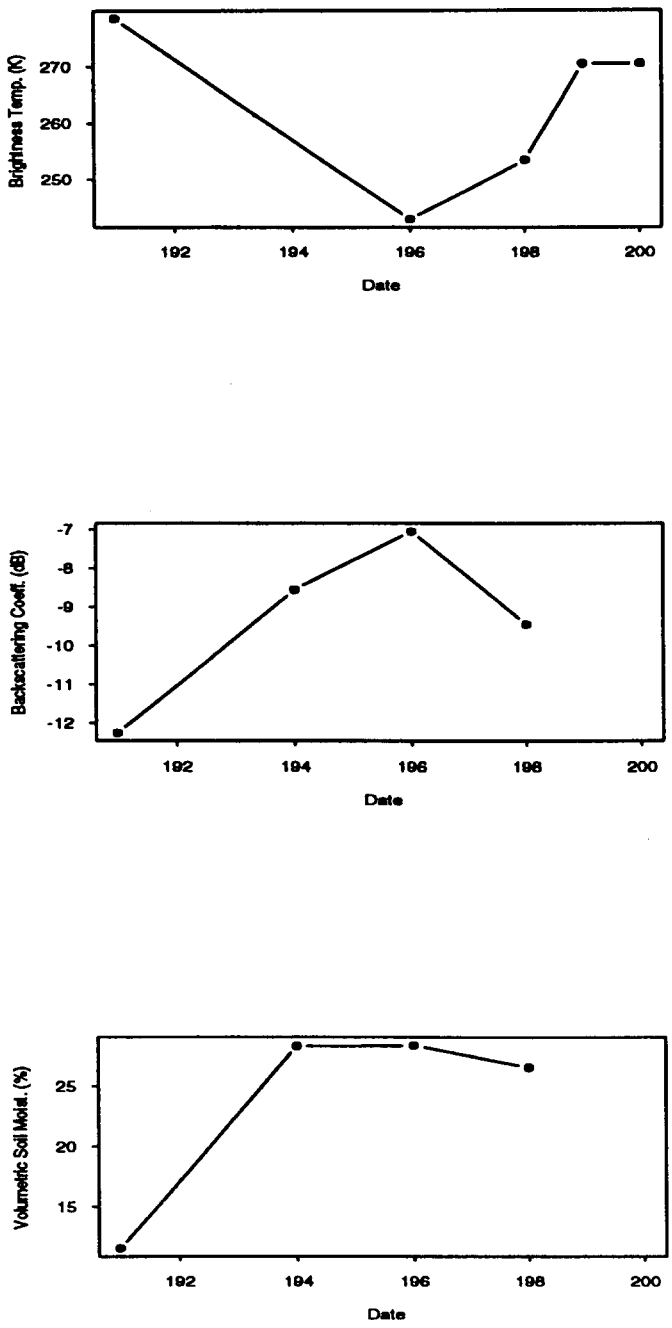

Figure 3: Temporal variation of brightness temperature and the L-band HH-polarization backscattering coefficient averaged over corn fields 1 and 2 during the course of the MACHYDRO'90 experiment. The local incidence angle of the SAR over corn fields 1 and 2 is approximately 39°.

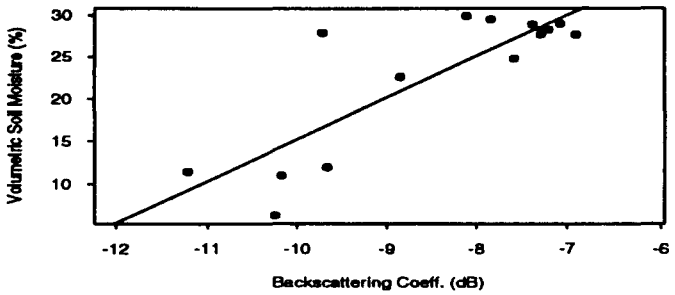

(a)

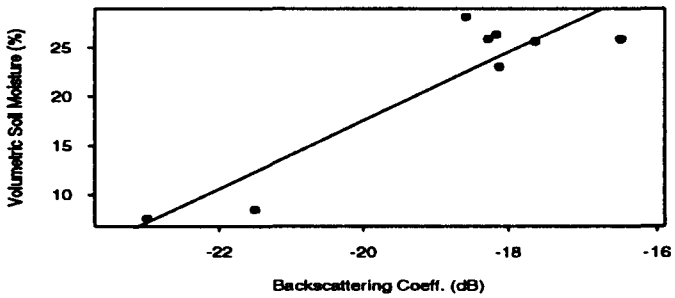

(b)

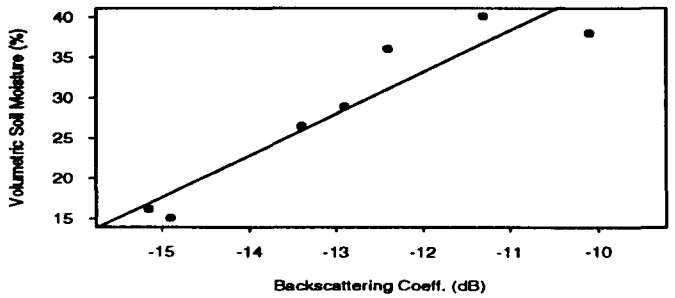

(c)

Figure 4: Regression relationships between the backscattering coefficients and the surface volumetric soil moisture contents for (a) corn fields, (b) oat fields, and (c) pasture areas.